

Uranium Electrodeposition Using Direct Potential Technique in Less Acidic Aqueous Media

A. M. Saliba-Silva^a, E. T. de Oliveira^a, M. Durazzo^a

^a Instituto de Pesquisas Energéticas e Nucleares
(Centro de Combustível Nuclear - IPEN/CNEN)
Av. Prof. Lineu Prestes, 2242 - São Paulo – SP – Brazil - CEP 05508-000
e-mail:saliba@ipen.br

Electrodeposition of uranium is a common practice to create samples for alpha spectrometry and it could be an alternative way to produce irradiation LEU targets to fabricate radiopharmaceuticals as ⁹⁹Mo used for cancer diagnosis. Usually electrodeposition of uranium uses ionic or aqueous solutions to produce uranium deposits in less acidic electrolytes (pH>2.5). During uranium electrodeposition, there is a high competition with H₂ evolution, once cathodic potentials are very high. In less acidic electrolyte the electrodeposition is uranyl hydroxyl and uranium oxides compounds, formed directly from uranyl (U-VI) structure. A reliable regression equation (R²=0.836) for alpha emission activity of uranium deposition was obtained, based on cell temperature and electrodeposition time. The deposition has oxide/hydroxide nature, acting as insulator during electrochemical process. The maximum level of deposited uranium, in terms of alpha activity, was around 34 Bq.cm⁻² (-1.8 V_{Ag/AgCl}, 2000 s, 60°C). In this condition, the inferred maximum amount of uranium was ~5.4 mg [U] /cm², which might be interesting to build probe samples to simulate irradiation targets.

Introduction

Electrodeposition of uranium is a common practice to create samples for alpha spectrometry (1) and this methodology could be an alternative way to produce irradiation LEU targets (2, 3) to fabricate radiopharmaceuticals as ⁹⁹Mo used for cancer diagnosis (4). Many workers (5) studied the uranium deposition at high temperature (>200°C) using salt baths and producing metallic uranium and alloys. The low temperature electrodeposition in ionic solutions is an ongoing investigation, mainly using RTIL way with moderate success as accounted in recent papers in the literature (6). Usually electrodeposition of uranium uses ionic or aqueous solutions to produce uranium deposits in less acidic electrolytes (pH>2.5). The performance of uranium electrodeposition is relatively erratic, since there is a high competition with H₂ evolution inside the reduction potential window. The technical literature is not stable in indicating a process for uranium electrodeposition to produce metallic uranium or other substances from the several uranium oxidation states. The aqueous route to produce metallic uranium appeared to have a marginal success, using high acidity (pH < 1) (7, 8). At pH>2, it is possible to deposit the oxidized uranium compound UO₂(OH)₂.H₂O as shown in the equilibrium diagram of molar fraction against pH presented in Figure 1(9).

Uranium electrodeposition at low temperature with direct polarization is a well-known technique (5, 10-19). Most of these used techniques of these experiments worked with well beyond equilibrium states. The uranium electrodeposition may be carried out using ionic or aqueous UO₂(NO₃)₂ solutions (12) with controlled acidity electrolytes (pH >2.5) to produce uranium hydroxide or oxide deposits (1). The performance of uranium electrodeposition is relatively low since there is

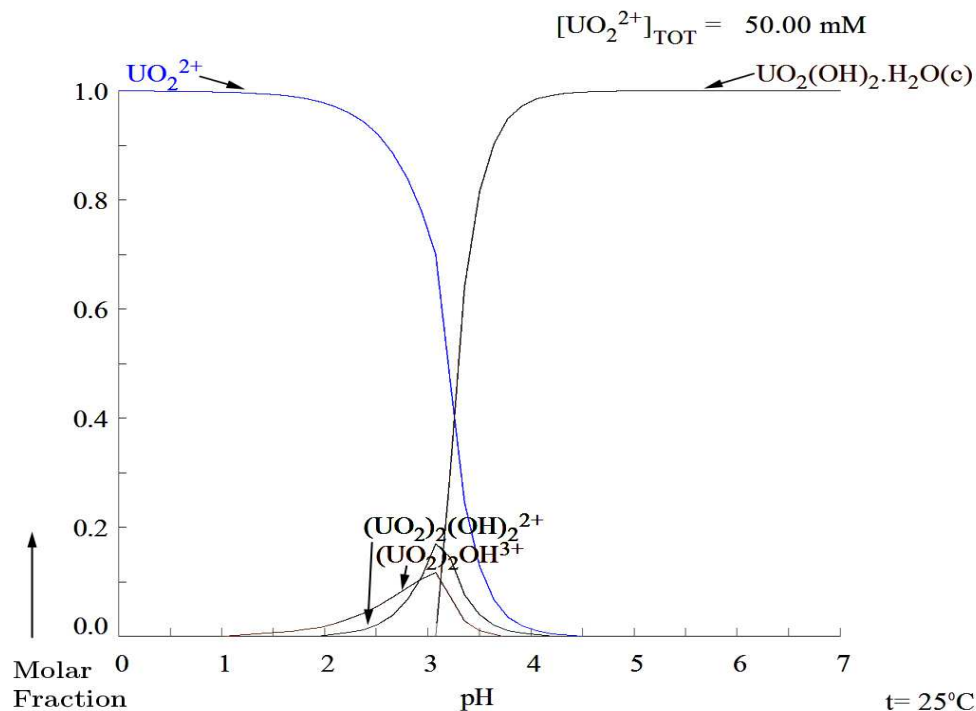


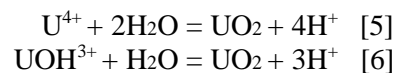
Figure 1. Equilibrium fraction diagram of $\text{UO}_2(\text{NO}_3)_2 \cdot 6\text{H}_2\text{O}$ solution with 50mM [U] against pH at 25°C, calculated by Medusa.

a big competition with H_2 reduction inside the potential window (1, 17, 18). Some publications deal with voltammetry analysis on uranium phenomena in ionic solutions with low pH, as reported by Rao et al. (20) claiming to have produced metallic uranium deposition, using MPPiNTf2 ionic solution. This route follows all reduction sequence of uranium-VI to metallic uranium, with the last reduction peak occurring at $-1.798 \text{ V}_{\text{SHE}}$. The window potential amplitude about uranium electrodeposition is quoted in US Patent 6,911,135 (5), reporting widespread range for uranium oxidation states reduction, from +1.5 to -2 V, when using electrolyte 1-butyl-2-methylimidazolium nitrate and 1-octyl-3-methylimidazolium chloride. Theoretically, in aqueous solution, using electrochemical reduction potential tables, for equilibrium states, it is indicated the following equations in cathodic direction (21):

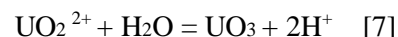


Interpreting this sequence, U(VI) and U(V) promptly transforms in U(IV), in cathodic field by reactions 1 and 2 and then reduced U(III) at $- 0.607 \text{ V}_{\text{SHE}}$ and to metallic U at $- 1.798 \text{ V}_{\text{SHE}}$. Shirasaki et al. (22), using dimethyl sulfoxide ionic solution, confirmed the sequence from uranium reduction from U(VI) to metallic uranium may happen. Giridar et al. (19) made electrochemical studies using the 1-butyl-2-methylimidazolium nitrate ionic solution and showed that UO_2 may be formed by an irreversible single step with two electron transfer, so not forming any metallic uranium and directly precipitating UO_2 as oxide or hydroxide. To have a technological electrodeposition of metallic uranium from low temperature aqueous or ionic electrolyte is fully desirable, nevertheless it does not seem to be an easy research and it is still in academic research field.

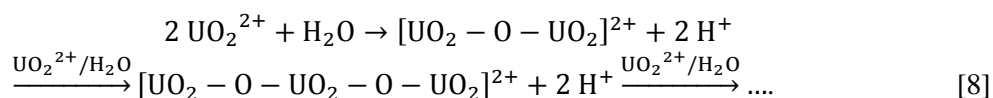
From experiments carried out by Giridhar et al. (19), their experiments, using 1-butyl-3-methylimidazolium chloride ionic solution, showed that at this region of cathodic potential, there might be reduction of U(VI) ($= \text{UO}_2^{2+}$) to U(IV) creating the possibility of UO_2 formation. The possible chemical reactions at this potential area are (23):



De Santos et al. (17), based on Wheeler et al. (24), did not find evidences of this reduction in less acidic media, stating that the deposited films were from U-VI oxide. Then, a possible chemical reaction would be:



They also suggested that, under hydrolysis and polymerization in less acidic media (pH~6), the material may develop the following chain reaction (24):



This precipitation would occur when the polymerization reaches the solubility product of the species in the electrolyte.

Experimental

The substrate preparation (nickel electrodeposition) and uranium electrodeposition used the same arrange, using AA 6061 aluminum alloy as coupons to prepare the substrate for nickel electrodeposition, over which a uranium electrodeposition was made. The electrochemical cell was a vertical quartz tube, supported by a polypropylene structure, containing the electrolyte solution inside the cell, which was sealed at the bottom exposing the cathode area (2 cm^2). Rubber O-ring covered with Teflon made the sealing. The used reference electrode was Ag/AgCl. One used a Metrohm Potenciostat 302SN. Figure 2 shows the actual cell used in the experiment.

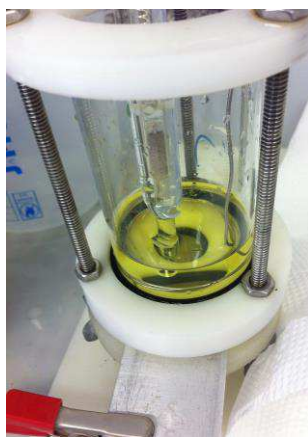


Figure 2. Actual electrochemical cell during uranium electrodeposition with uranyl electrolyte.

Ni-substrate. The AA6061 coupons (20 mm x 20 mm) were heat treated at 450°C during 1 hour, and ground with emery paper #600, rinsed at 2M NaOH for 2 minutes and duly degreased with acetone. All aluminum coupons were electroplated by nickel electrolyte (Watt's

bath: 0.85 mol.L⁻¹ NiSO₄.6H₂O + 0.15 mol.L⁻¹ NiCl₂ + 36g.L⁻¹ H₃PO₄ with pH = 3.7; -1.5 V_{Ag/AgCl}; 600s; counter-electrode: electrolytic nickel). The prepared nickel substrate was then degreased with acetone.

Uranium Electrodeposition. The used uranyl aqueous solution was a homemade nuclear pure UO₂(NO₃)₂.6H₂O diluted in deionized water to 50mM [U], having a natural pH at 2.6. The experiments had two temperature levels at 30°C and 60°C. The electrodeposition times were 600, 1000, 1500 and 2000 s. The cathodic potential was kept constant at -1.80 V_{Ag/AgCl}. Each experiment used a 30 ml volume of fresh uranyl solution to perform the uranium electrodeposition. The counter electrode was Pt-wire, with enough reaction area in order to avoid restriction of evolving reactions. A following-up statistical fitting analysis of the alpha emission activity allowed an indirect information of uranium mass deposition.

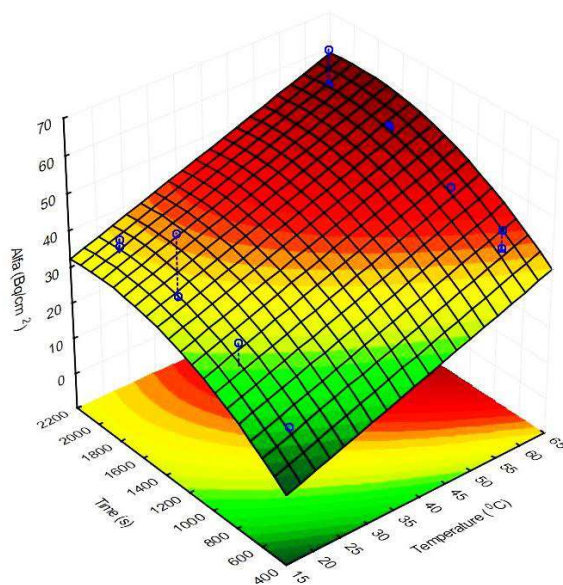
Results and Discussion

Table 1 shows the summary of the results obtained from the electrochemical deposition of uranium. As shown in this table, the main factors were temperature in Celsius and time in seconds. The dependent variable was ALPHA, the radioactivity of alpha emission developed in the sample after the uranium electrodeposition, in Bq/cm².

Table 1. Results of uranium electrodeposition experiment.

Experiment	Pot (V)	Temperature (C)	Time (s)	ALPHA (Bq/cm ²)
E30719A	-1.80	30	600	14.25
E30719B	-1.80	30	600	19.47
E30719C	-1.80	30	600	14.00
E30722A	-1.80	30	1000	23.46
E30722B	-1.80	30	1000	32.80
E30722C	-1.80	30	1000	23.36
E30725A	-1.80	30	1500	23.27
E30725B	-1.80	30	1500	34.23
E30725C	-1.80	30	1500	51.03
E30726A	-1.80	30	2000	28.30
E30726B	-1.80	30	2000	38.66
E30726C	-1.80	30	2000	36.97
E30730A	-1.80	60	600	40.65
E30730B	-1.80	60	600	45.46
E30730C	-1.80	60	600	39.31
E30731A	-1.80	60	1000	41.09
E30731B	-1.80	60	1000	48.81
E30731C	-1.80	60	1000	45.37
E30801A	-1.80	60	1500	54.45
E30801B	-1.80	60	1500	55.39
E30801C	-1.80	60	1500	53.81
E30802D	-1.80	60	2000	56.81
E30805A	-1.80	60	2000	54.34
E30805B	-1.80	60	2000	66.45
E30805C	-1.80	60	2000	49.40

Figure 3 shows a 3D-graph and concerned surface fitting data of the results. As could be seen, the results have an adequate statistical significance for the response surface fitting, giving then a prediction equation of experimental data range.



$R^2 = 0.836$	Reg.Coeff.	Std.Err.	t-student	p-value	-95%	95%
Intercept	12.1749	9.4705	-1.2856	0.2126	-31.8700	7.5201
Temp (L)	0.5309	0.0626	8.4808	0.0000	0.4007	0.6611
Time (L)	0.0378	0.0156	2.4226	0.0245	0.0054	0.0703
Time (Q)	-9.66E-06	5.88E-06	-1.6432	0.1152	-2.19E-05	2.57E-06

Figure 3. Adjusted 3D surface to the variation of alfa activity (Bq/cm^2) of uranium electrodeposition over nickel substrate with temperature and time. The table shows the statistical indications of the surface quadratic fitting.

The deposition over the substrate has a grayish deposit of uranium substance, which is adherent to the substrate, as shows Figure 4 with a typical macroscopic appearance of U-deposition. Some protuberances appears over the deposition layer, which may be seen in detail in SEM microstructure as bushes or sponges. They are thought to be also part of uranium deposition, but in a different evolution process occurring after the initial coverage of uranium material. The cracking formation over the structure, as could be seen in Figure 4B, which occurs in the microstructures, happened not during deposition itself, but during sample drying. It revealed that the formed deposition film is very fragile once dried. The dehydration and crystallographic building-up of the uranium deposit is an ongoing research of this researchers' group.

The suggested polymerization under hydrolysis, as delineated by De Santos et al. (17) and Wheeler et al. (24), seems to be a good explanation for the structure development of uranium electrodeposition, as a uranyl hydroxide/uranium oxide formation. Nevertheless, this model delineated by this authors for electrolytes with $pH > 4$, seems to be valid at lower pHs (< 3), where water hydrolysis would have another acidic expected reactions. Probably, localized areas in the cathode may behave as anodic sites producing hydroxyl anions. Most likely, the electrodeposition

in less acidic electrolyte forms uranyl hydroxyl and uranium oxides compounds at the cathode surface, direct from uranyl (Uranium-VI), without redox reactions of uranium oxidation states.

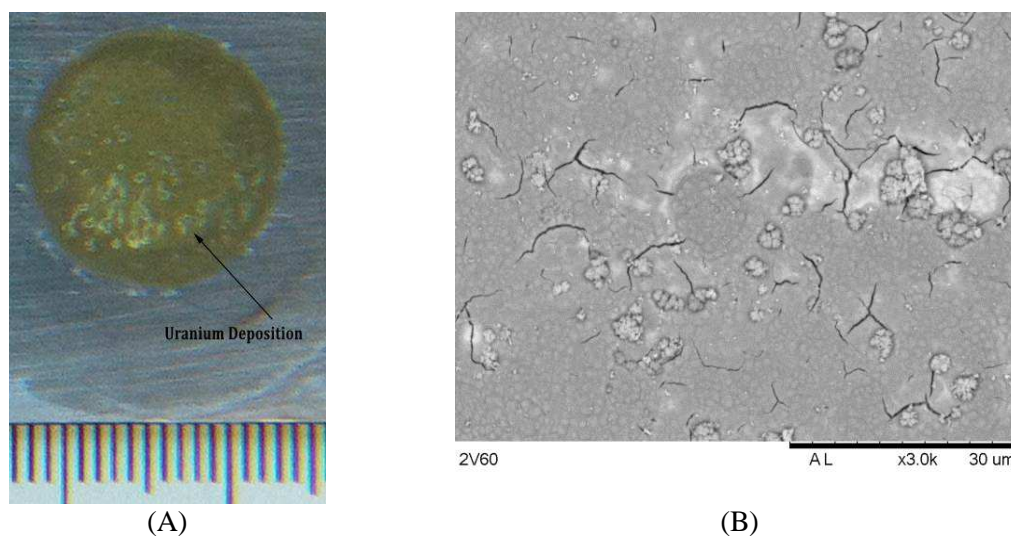


Figure 4. (A) Macroscopic view of uranium electrodeposit over nickel substrate. (B) Typical SEM micrograph showing the coverage of uranium substance.

In this work, we aimed to achieve higher uranium mass deposition amount in a shorter time, since this is crucial for technological reasons to produce targets. From the analyzed experimental results, we arrived to a polynomial equation to represent the growth in alpha activity, so in uranium content, depending on the electrolyte temperature, inside the range 30-60°C, and the electro-deposition time in the range 600-2000 s. One can write this surface response equation in the following form:

$$\frac{d \text{ALPHA}}{dt} = -12.175 + 0.531 \cdot T + 0.0378 \cdot t - 9.66 \cdot 10^{-6} \cdot t^2 \quad [9]$$

Where ALPHA represents the alpha activity of the deposit, T is the temperature in Celsius and t is the electro-deposition time in seconds. Note that the last term of this equation has a negative coefficient of a quadratic influence for electro-deposition time. This influence is important and coherent with the deceleration in deposit amount as the deposition time increases. Statistics of this coefficient is not as significant as the other coefficients for this equation, but the level of error, for accepting it, is around 11%, which is fair for considering it as a valid coefficient. This indicates the deceleration of the process seems to occur caused by the properties of deposited layer of uranium compound as an insulator to the charge transfer at the cathode.

Figure 5 presents the direct current evolution during uranium electro-deposition at cathodic potential -1.8 V, working with cell temperatures at 30°C and 60 °C. It shows that the process of uranium electro-deposition is thermal energy driven, since the involved amount of consumed electrical charge increased and so the U-deposit thickened with temperature. One can also observe this phenomenon in Figure 3. One can also estimate the amount of deposited uranium by alpha-activity as 12.31 Bq by one milligram of ^{238}U . Therefore, the estimated uranium deposition in the experiments would be no more than 5.4 mg [U] for the sample E30805B in Table 1. By Faraday's law, given by the following equation:

$$m = \frac{Q \cdot M}{F \cdot z} \quad [10]$$

where m is the substance mass, Q is the consumed charge in Coulombs, F is Faraday's number 96485.34, M is the substance molar mass, z is the number of electrons transferred for each ion.

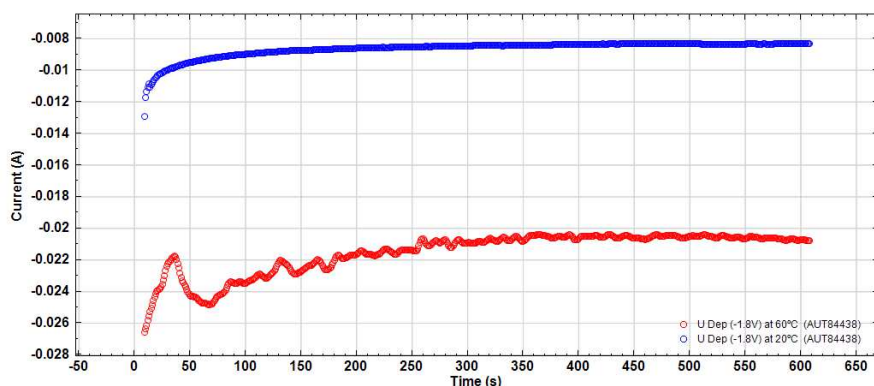


Figure 5. Evolution of current density during uranium electrodeposition at 30°C and 60°C, from $\text{UO}_2(\text{NO}_3)_2$ 50mM aqueous electrolyte (pH 2.6) at cathodic potential -1.8 V. The electrochemical cell suffered no stirring during the process.

Considering two involved electrons to reduce UO_2^{2+} , the integration of current versus time curve for a full period of 2000 s, gave a consumed charge of -40.5 coulombs. Then, the expected amount of deposited uranium, without any H_2 evolution would be around 50 mg of uranium over the sample.

Considering that the U-deposit amount is 5.4 mg, as estimated above, it gives a proportion of 50/5.4, which is almost 10 times more than the necessary charge to produce uranyl deposition. This level is far beyond the present experiment result; consequently, the other reduction in competition to uranium deposition was the evolution of H_2 , which accounted with 9:1 electrons compared to uranyl deposition. Therefore, the major amount of charge consumption is due to hydrogen evolution at the cathode. Nevertheless, these chronoamperometric measures gave a decreasing tendency for current as the electrodeposition takes place. The authors related this effect to the deposit of oxide/hydroxide layer, which is less electrically conductive. As the regular layer thickens, it provides a continuous increase in electrical resistance, then impeding the electrodeposition reaction and H_2 evolution to take place.

Conclusion

Uranium electrochemistry and its various redox reactions promote a complex picture of possible reactions. These reactions may vary due to different electrolytes and electrochemical conditions. Most likely, in less acidic electrolyte (pH~2.6), the electrodeposition formation at the cathode surface is uranyl hydroxyl associated to uranium oxides substances, which were formed directly from uranyl (Uranium-VI) structure. There was a significant increase in cathodic electrical resistance, which lowered gradually as the electrodeposition happened. This endorses the U-deposition as having the oxide/hydroxide nature, which acted as insulator during the electrochemical reactions taking place. From experiment results, the maximum level of uranium deposition rate, obtained by DC polarization (2000 s, -1.8 $\text{V}_{\text{Ag}/\text{AgCl}}$; 60°C) was around 34 $\text{Bq}\cdot\text{cm}^{-2}$. The experimental results allowed obtaining a reliable regression equation for response surface of alpha activity based on cell temperature (linear) and electrodeposition time (linear and quadratic). The amount of uranium mass, in maximum alpha conditions, was ~5.4 mg [U] / cm^2 , which might be interesting to build probe samples to simulate irradiation targets.

Acknowledgement

Thanks are due to FAPESP for granting this research by the project PJ-2013/08514-3. Thanks are also due to the laboratories from Nuclear Fuel Center from IPEN/CNEN-SP and its staff.

References

1. M.T. Crespo, *Appl Radiat Isot.* **70**(1): p.: 210. (2012).
2. A.M. Saliba-Silva, et al., *ECS Meeting Abstracts*(25): p.: 999. (2012).
3. A.M. Saliba-Silva, et al., *2011 Int. Nuclear Atlantic Conference*: p. (2011).
4. C. National Research Council, *Medical isotope production without highly enriched uranium*, C. National Research Council, Editor. 2009, National Academies Press.
5. R.C. Thied, et al., *Process for separating metals - US 6,911,135*, in *United States Patent*, U.S. Patent, Editor. 2005: US.
6. P. Giridhar, et al., *Journal of Alloys and Compounds.* **448**(1-2): p.: 104. (2008).
7. A. Saliba-Silva, et al., *Electrochemical Studies on 99Mo Target Materials: Acidic Deposition of Uranium Compounds.*, in *RERTR 2012 - 34th Int. Meeting on Reduced Enrichment for Research and Test Reactors*. 2012, DOE/Argonne National Lab/RERTR.
8. A.M. Saliba-Silva, et al., *ECS Meeting Abstracts*(25): p.: 1002. (2013).
9. I. Puigdomenech, *MEDUSA*. 2009, Royal Institute of Technology: Stockholm, Sweden. p. Software to calculate equilibrium diagrams.
10. S. Prakash, et al., *International Journal of Applied Radiation and Isotopes.* **22**: p.: 128. (1971).
11. M.V. Ramaniah, et al., *Intern. J. Appl. Rad. and Isot.* **26**: p.: 648. (1975).
12. L. Hallstadius, *Nuclear Instruments & Methods.* **223**: p.: 266. (1984).
13. Y.V. Lobanov, et al., *Nuclear Instruments & Methods in Physics Research.* **397**: p.: 26. (1997).
14. D. Luna-Zaragoza and J. Serrano G., *Applied Radiation and Isotopes.* **51**: p.: 499. (1999).
15. M.H. Lee and C.W. Lee, *Nuclear Instruments and Methods in Physics Research A.* **447**: p.: 8. (2000).
16. F. Miserque, et al., *Journal of Nuclear Materials.* **298**: p.: 280. (2001).
17. R.N. Dos Santos, L.S. Marques, and F.B. Ribeiro, *Applied Radiation and Isotopes.* **56**(5): p.: 741. (2002).
18. K. Eberhardt, et al., *Nuclear Instruments and Methods in Physics Research Section A: Accelerators, Spectrometers, Detectors and Associated Equipment.* **521**(1): p.: 208. (2004).
19. P. Giridhar, et al., *Electrochimica Acta.* **52**(9): p.: 3006. (2007).
20. C. Jagadeeswara Rao, et al., *Journal of Nuclear Materials.* **408**(1): p.: 25. (2011).
21. D.R. Lide, *CRC Handbook of Chemistry and Physics (87th ed.)*. 2006, Boca Raton, FL: CRS Press.
22. K. Shirasaki, et al., *Journal of Alloys and Compounds.* **418**(1-2): p.: 217. (2006).
23. Y. Xu, *Electrochemical Treatment of Metal-Bearing Aqueous Waste Based on Novel Forms of Carbon*, in *College of Engineering and Mineral Resources 1999*, West Virginia University: Morgantown, Vi.
24. V.J. Wheeler, R.M. Dell, and E. Wait, *Journal of Inorganic and Nuclear Chemistry.* **26**(11): p.: 1829. (1964).